Statistics of electromagnetic transitions as a signature of chaos in many-electron atoms

V. V. Flambaum, A. A. Gribakina, and G. F. Gribakin
School of Physics, University of New South Wales, Sydney 2052, Australia
(Received 28 January 1998)

Using a configuration-interaction approach, we study statistics of the dipole matrix elements ($E1$ amplitudes) between the 14 lower states with $J^{\pi}=4^{-}$ and 21st to 100th even states with $J=4$ in the Ce atom (1120 lines). We show that the distribution of the matrix elements is close to Gaussian, although the width of the Gaussian distribution, i.e., the root-mean-square matrix element, changes with the excitation energy. The corresponding line strengths are distributed according to the Porter-Thomas law which describes statistics of transition strengths between chaotic states in compound nuclei. We also show how to use a statistical theory to calculate mean-squared values of the matrix elements or transition amplitudes between chaotic many-body states. We draw some support for our conclusions from the analysis of the 228 experimental line strengths in Ce [J. Opt. Soc. Am. **8**, 1545 (1991)], although direct comparison with the calculations is impeded by incompleteness of the experimental data. Nevertheless, the statistics observed give evidence that highly excited many-electron states in atoms are indeed chaotic.
[S1050-2947(98)04207-3]

PACS number(s): 31.10.+z, 32.70.Cs, 31.50.+w, 05.45.+b

I. INTRODUCTION

The aim of this work is to present more evidence that excitation spectra of complex open-shell atoms, and probably any other atom at sufficient excitation energies, display clear quantum chaotic features. This phenomenon is caused by strong mixing of many-electron excited states by the residual two-body Coulomb interaction. It manifests itself, in particular, in Gaussian statistics of the $E1$ amplitudes for these states.

Since the time of Bohr's hydrogen atom theory, atoms were considered as perfectly regular dynamical systems. As the classical theory of chaos evolved, it became apparent that highly excited atomic states in the Rydberg range could become chaotic if an external field is applied [1], as long as the underlying classical motion is chaotic.

On the other hand, it was also due to Bohr that the notion of compound nuclei was introduced in physics. The behavior of these highly excited nuclear states is essentially quantum mechanical. Nevertheless, they display a number of chaotic properties. For example, the statistics of their energy spectra show certain universal features, and transition amplitudes involving compound states obey Gaussian statistics [2]. To describe these properties, it was suggested by Wigner that the Hamiltonian of a compound nucleus could be modeled by a random matrix, and different characteristics found by averaging over ensembles of such matrices (see Refs. [3,4]).

The first insight into quantum chaotic properties of complex atoms was given by Rosenzweig and Porter [5], who analyzed experimental spectra of some neutral atoms, and showed that in heavy open-shell atoms the spectral statistics are similar to those of compound nuclei. That analysis was later extended and refined in Ref. [6]. Of course, the study of eigenvalues provides valuable information about the system. On the other hand, the spectral statistics observed in heavy open-shell atoms are similar to those of the hydrogen atom in a strong magnetic field [7], or even a particle in a two-dimensional classically ergodic billiard [8]. However, the eigenstates of these quantum systems must be completely different, and it is clear that the eigenvalue statistics cannot really tell us much about the origin of chaotic behavior, or indeed the structure of the chaotic eigenstates.

The first inquiry into the possibility of chaos in the eigenstates of complex atoms was done by Chirikov [9]. He studied configuration compositions of eigenstates of the Ce atom using data from tables [10], and came to the conclusion that ''eigenfunctions are random superpositions of some few basic states.'' Inspired by that work, we conducted an extensive numerical study of the spectra and eigenstates of complex open-shell atoms, using the rare-earth atom of Ce as an example [11–13]. This allowed us to investigate many-body quantum chaos in a real system. We showed that atomic excited states are in fact similar to nuclear compound states, and developed a statistical approach for analyzing their properties.

Unlike eigenvalues, the eigenfunctions are not observable directly. To probe the structure of the chaotic eigenstates, one can look at the transition probabilities or matrix elements of some external perturbation coupling them to each other, or to regular, simple eigenstates (like the ground state). The matrix elements involving chaotic eigenstates must have Gaussian statistics. We showed that its main characteristics — the mean-squared value of the matrix element between the chaotic multiparticle states (compound states) — can be calculated in terms of statistical parameters of the eigenstates and single-particle amplitudes and occupation numbers of the orbitals present in the compound states [11,14].

In this work we have chosen the quantity most easily accessible experimentally — the $E1$ amplitudes. This also gives us an opportunity to look for experimental signatures of chaos in the Ce atom using the work by Bisson *et al.* [15], where over 200 line strengths were measured for transitions between a large number of levels within 3.5 eV of the ground state. It should be mentioned that there are many other possible atomic systems to search for quantum chaos, e.g., in doubly excited states and inner-shell excitation spec-

tra of alkaline-earth atoms [16–18], or even multiply excited states of light atoms [19].

Chaotic many-body states

Let us now recall briefly what chaotic many-electron atomic eigenstates are. Suppose one uses a basis of some single-electron orbitals (e.g., the Hartree-Fock ones) to construct many-electron basis states $|\Phi_k\rangle$. The states $|\Phi_k\rangle$ can be taken as single-determinant states corresponding to certain configurations of a few valence electrons, or constructed from them through some coupling scheme to be of definite total angular momentum J. The true atomic eigenstates

$$|\Psi_i\rangle=\sum_k C_k^{(i)}|\Phi_k\rangle \quad \left(\sum_k C_k^{(i)2}=1\right) \tag{1}$$

and eigenvalues $E^{(i)}$ are obtained by diagonalizing the Hamiltonian matrix $H_{jk}\equiv\langle\Phi_j|\hat{H}|\Phi_k\rangle$. The coefficients $C_k^{(i)}$ describe mixing of the basis states by the residual Coulomb interaction. In the multielectron excitation range the number of basis states $|\Phi_k\rangle$ formed by distributing several electrons among a few open orbitals is large. Many of these states are nearly degenerate, and the mean spacing between the basis state energies $E_k\equiv H_{kk}$ is likely to be smaller than the typical value of the off-diagonal matrix element H_{jk}. In this situation the basis states are strongly mixed together [20].

Apart from a few lowest levels, each of the eigenstates is a superposition of a large number of basis states. Of course, by a simple perturbation theory argument, the mixing must be weak for distant basis states (large $|E_j-E_k|$). The strong mixing takes place within a certain energy range $|E_j-E_k| \lesssim \Gamma=2\pi V^2/D$, where D is the mean level spacing, $V^2=\overline{H_{jk}^2}$, and Γ is called the *spreading width*, since it characterizes the spread of the eigenstates to which a given basis state contributes noticeably. One can estimate the number of *principal components*, i.e., those that contribute significantly to a given eigenstate (1), as $N\sim\Gamma/D$. The coefficients $C_k^{(i)}$ corresponding to the principal components have typical values $|C_k^{(i)}|\sim 1/\sqrt{N}$. Their statistics is close to that of independent random variables, and tends toward Gaussian when the mixing is strong. In this case even the single-electron orbital occupancies are far from integer and only the total angular momentum, the parity, and the energy itself remain good quantum numbers [11]. Thus we can talk about *quantum chaos* in the system. This situation is similar to that in compound nuclei, and the corresponding chaotic eigenstates can be called atomic compound states. The model configuration-interaction calculations performed for Ce produced a value of $\Gamma\sim 2$ eV, and demonstrated the existence of a dense spectrum of chaotic compound excited states with $N\gtrsim 100$ ($D\sim 0.01$ eV) just few eV from the ground state [11].

II. MATRIX ELEMENTS BETWEEN CHAOTIC STATES

Consider two chaotic many-body states (compound states, for short) that are superpositions of large numbers of basis states, $|\Psi_1\rangle=\Sigma_k C_k^{(1)}|\Phi_k\rangle$ and $|\Psi_2\rangle=\Sigma_j C_j^{(2)}|\Phi_j\rangle$. If the expansion coefficients $C_k^{(i)}$ are random, the matrix element of some operator $\hat{M}$

$$\langle\Psi_2|\hat{M}|\Psi_1\rangle=\sum_{jk} C_j^{(2)}\langle\Phi_j|\hat{M}|\Phi_k\rangle C_k^{(1)} \tag{2}$$

is a sum of a large number of almost uncorrelated random items [21]. Therefore, one should expect that such matrix elements display Gaussian statistics with zero mean. Hence the probability distribution of the matrix elements between compound states can be characterized by their mean-squared value alone.

If $\hat{M}$ is a single-particle operator, e.g., the electric dipole moment $\hat{D}=\Sigma_{\alpha\beta}\langle\alpha|d|\beta\rangle a_\alpha^\dagger a_\beta$ (α and β are single-particle states), it is convenient to express its matrix elements in terms of the matrix elements of the density matrix operator $\hat{\rho}_{\alpha\beta}=a_\alpha^\dagger a_\beta$,

$$\langle\Psi_2|\hat{D}|\Psi_1\rangle=\sum_{\alpha\beta}\langle\alpha|d|\beta\rangle\langle\Psi_2|a_\alpha^\dagger a_\beta|\Psi_1\rangle=\sum_{\alpha\beta} d_{\alpha\beta}\rho_{\alpha\beta}^{(21)}, \tag{3}$$

where $\rho_{\alpha\beta}^{(21)}\equiv\langle\Psi_2|\hat{\rho}_{\alpha\beta}|\Psi_1\rangle$.

In Refs. [14] and [11] a statistical approach to the calculation of mean-squared matrix elements between compound states was developed. It is first based on the assumption that contributions from different single-particle transitions $\beta\to\alpha$ in the matrix element (3) are uncorrelated. The mean-squared value is then given by

$$\overline{|\langle\Psi_2|\hat{D}|\Psi_1\rangle|^2}=\sum_{\alpha\beta}|d_{\alpha\beta}|^2\overline{|\rho_{\alpha\beta}^{(21)}|^2}, \tag{4}$$

where averaging is done over a number of compound states around Ψ_1 and/or Ψ_2. The mean-squared value of the density-matrix operator $\overline{|\rho_{\alpha\beta}^{(21)}|^2}$ is expressed in terms of the parameters of the compound states 1 and 2 (i.e., their energies and spreading widths), and the average occupation numbers of the single-particle states α and β.

In a spherically symmetric system where the states 1 and 2 are characterized by their total angular momenta $J_{1,2}$ and projections $M_{1,2}$, the Wigner-Eckhart theorem applies, and it is convenient to deal with the reduced matrix elements $\langle\Psi_2\|\hat{D}\|\Psi_1\rangle$ independent of the projections $M_{1,2}$. For example, the mean-squared value of the zero-rank reduced density matrix operator ($J_1=J_2\equiv J$ then) is obtained in the following two forms [11]:

$$\overline{|\rho_{nlj,n'l'j}^{(21)0}|^2} = \begin{cases} D_1\tilde{\delta}(\Gamma_1,\Gamma_2,\Delta)\left(\dfrac{2J+1}{2j+1}\right)\left\langle n_{nlj}\left(1-\dfrac{n_{n'l'j}}{2j+1}\right)\right\rangle_2 \\ D_2\tilde{\delta}(\Gamma_1,\Gamma_2,\Delta)\left(\dfrac{2J+1}{2j+1}\right)\left\langle n_{n'l'j}\left(1-\dfrac{n_{nlj}}{2j+1}\right)\right\rangle_1 \end{cases}, \tag{5}$$

where $D_{1,2}$ are the mean level spacings near the states 1 and 2, n_{nlj} and $n_{n'l'j}$ are the orbital occupation numbers, and $\tilde{\delta}$ is a ''finite-width δ function.'' It depends on the spreading

widths $\Gamma_{1,2}$ of the compound states and on the energy difference $\Delta=\omega_{n'l'j,nlj}-E^{(1)}+E^{(2)}$ between the transition frequency for the compound many-electron states $E^{(1)}-E^{(2)}$ and the frequency $\omega_{n'l'j,nlj}$ of the single-particle transition between the orbitals nlj and $n'l'j$. The function $\tilde{\delta}$ has a maximum at $\Delta=0$, and describes the energy conservation for the compound states. Its width is determined by the spreading widths $\Gamma_{1,2}$. Note that $\langle\cdots\rangle_{1,2}$ in Eq. (5) denotes averaging of the occupation-number factors over the compound states 1 or 2. Note also that the exact form of the function $\tilde{\delta}(\Gamma_1,\Gamma_2,\Delta)$ depends on the spreading of the compound states over the basis components, i.e., on the ''shapes'' of the eigenstates. In the simplest approximation this spreading is described by the Breit-Wigner formula (see numerical studies in Ref. [11]), and $\tilde{\delta}$ is also a Breit-Wigner profile

$$\tilde{\delta}(\Gamma_1,\Gamma_2,\Delta)=\frac{1}{2\pi}\frac{\Gamma_1+\Gamma_2}{\Delta^2+(\Gamma_1+\Gamma_2)^2/4}. \tag{6}$$

To calculate the mean-squared value of the $E1$ amplitude, we now need a formula for the reduced density-matrix operator of the first rank. Starting from the definition [11]

$$\rho^{(21)1}_{nlj,n'l'j'}=(-1)^{J_2-M_2}\begin{pmatrix} J_2 & 1 & J_1 \\ -M_2 & q & M_1\end{pmatrix}^{-1} \times\sum_{mm'}(-1)^{j-m}\begin{pmatrix} j & 1 & j' \\ -m & q & m'\end{pmatrix}\rho^{(21)}_{nljm,n'l'j'm'} \tag{7}$$

for $q=0$ (linear polarization along the quantization axis), and assuming that transitions between different magnetic sublevels m are uncorrelated, we can derive a formula for the mean square of Eq. (7), and then use it to obtain the mean-squared $E1$ amplitude

$$\overline{|\langle\Psi_2\|\hat{D}\|\Psi_1\rangle|^2}=\frac{2J_1+1}{3}D_2\sum_{nlj,n'l'j'}|\langle nlj\|d\|n'l'j'\rangle|^2 \times\tilde{\delta}(\Gamma_1,\Gamma_2,\Delta)\left\langle\frac{n_{n'l'j'}}{2j'+1}\left(1-\frac{n_{nlj}}{2j+1}\right)\right\rangle_1, \tag{8}$$

analogous to the lower formula in Eq. (5), or an alternative form with D_1 and $\langle n_{nlj}/(2j+1)\,(1-[n_{n'l'j'}/(2j'+1)])\rangle_2$ on the right-hand side. The factor $\frac{1}{3}$ on the right-hand side of Eq. (8) is due to the fact that there are three final-state momenta $J_2=J_1$ and $J_1\pm1$ accessible from a given J_1 by means of a dipole transition. In deriving this expression, an additional assumption has been made that the occupancies of the $nljm$ and $n'l'j'm'$ states are statistically independent, and the states with different m within the same nlj shell are equally populated. This supposition influences only the ''emptiness'' factors $(1-[n_{nlj}/(2j+1)])$, which are close to unity anyway when the number of single-electron states available is much greater than the number of active electrons.

The square of the reduced dipole matrix element $S(2,1)=|\langle\Psi_2\|\hat{D}\|\Psi_1\rangle|^2$ is called the strength of the line $1\to2$, so Eq. (8) allows one to estimate *mean line strengths* for transitions involving compound states.

It is interesting to note that the statistical theory expression (8) satisfies the dipole sum rule [26] (in atomic units)

$$\frac{2}{3}\sum_{J_2,E^{(2)}}\frac{E^{(2)}-E^{(1)}}{2J_1+1}|\langle\Psi_2\|\hat{D}\|\Psi_1\rangle|^2\approx n, \tag{9}$$

where n is the number of active valence electrons included in the configuration space of the problem. To obtain this result, one should replace summation over the final states 2 with integration over $dE^{(2)}/D_2$, take into account that $\int(E^{(2)}-E^{(1)})\tilde{\delta}(\Gamma_1,\Gamma_2,\Delta)dE^{(2)}=\omega_{nlj,n'l'j'}$ [see Eq. (6)], neglect the ''emptiness'' factor $(1-[n_{nlj}/(2j+1)])\approx1$, use $\Sigma_{n'l'j'}\langle n_{n'l'j'}\rangle_1=n$, and rely on the single-particle sum rules for the orbitals $n'l'j'$ occupied in the initial state Ψ_1,

$$\frac{2}{3}\sum_{nlj}\frac{\omega_{nlj,n'l'j'}}{2j'+1}|\langle nlj\|d\|n'l'j'\rangle|^2\approx1. \tag{10}$$

III. NUMERICAL RESULTS FOR THE CE ATOM

A. Energy levels

Cerium, $Z=58$, is the second of the lanthanide atoms. Its electronic structure consists of the Xe-like $1s^2\ldots5p^6$ core and four valence electrons. The atomic ground state is described by the $4f6s^25d$ configuration with $J^\pi=4^-$ [10].

The origin of the extremely complex and dense excitation spectra of the rare-earth atoms is the existence of several open orbitals near the ground state, namely, $4f$, $6s$, $5d$, and $6p$, or, in relativistic notation, $4f_{5/2}$, $4f_{7/2}$, $6s_{1/2}$, $5d_{3/2}$, $5d_{5/2}$, $6p_{1/2}$, and $6p_{3/2}$. These make a total of $N_s=32$ single-electron states. For Ce with $n=4$ valence electrons, there are about $(N_s)^n/n!\approx4\times10^4$ possible many-electron states constructed of them. If we allow for two possible parities, about ten possible total angular momenta J, and $2J+1$ different projections (another factor of 10), there will be still hundreds of energy levels within a given J^π manifold.

In the present work we perform relativistic configuration-interaction calculations in the Hartree-Fock-Dirac basis analogous to those in Ref. [11]. In that work, we limited ourselves to just seven nonrelativistic configurations constructed of the $4f$, $6s$, $5d$, and $6p$ orbitals, for both odd and even states, which produced 260 and 276 states with $J^\pi=4^-$ and 4^+, respectively. To make the results more realistic, we have extended the configuration basis set by nine odd and 23 even nonrelativistic configurations. Basically, the additional configurations were obtained by exciting one of the four electrons of an ''old'' configuration into the next orbital, e.g., the lowest even $4f^26s^2$ configuration would produce $4f6s^25f$, $4f6s^27p$, $4f^26s7s$, and $4f^26s6d$ configurations. To keep the size of the configuration space reasonable, we included only the configurations with mean energies within about 10 eV from the Ce ground state. This increased the total number of 4^- and 4^+ states to 862 and 1433, respectively. Note that $J=4$ states have been chosen because these manifolds are among the most abundant.

As a result, the level density $\rho(E)=\Sigma_i\delta(E-E^{(i)})$ has increased greatly above 4 eV and become closer to that observed experimentally. Of course, to be meaningful, the level

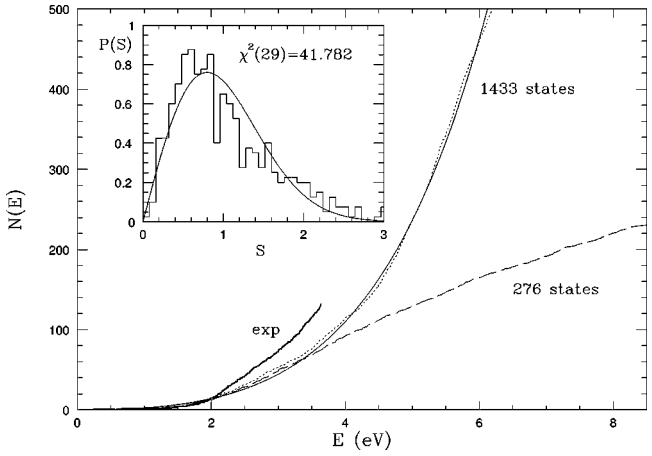

FIG. 1. Energy spectra and level statistics of the $J^\pi=4^+$ states in Ce. The dashed line shows the cumulative number of states $N(E)$ for the calculation with 276 basis states [11]; the dotted line is the present calculation with 1433 basis states; the thick solid line is $N(E)$ for 132 experimental levels from Ref. [10]. The thin solid line is the cumulative level number corresponding to the independent-particle fit (13). Shown in the inset are the statistics of the normalized level spacings s for the lowest 500 levels, compared with the Wigner distribution (14).

density must be averaged over some small energy interval to obtain a smooth function rather than a set of spikes. An alternative procedure is to look at the cumulative number of levels

$$N(E)=\int_{-\infty}^{E}\rho(E')dE', \tag{11}$$

which we present in Fig. 1 for $J^\pi=4^+$ states. Each $N(E)$ plot is a staircase of steps of the unit height occurring at successive excited state energies. The level density can be easily estimated from the slope of the $N(E)$ plot. The experimental data for the 132 even levels with $J=4$ known from Ref. [10] is shown by the solid-line staircase, and the energies are given with respect to either the experimental or calculated ground-state energy. They can be compared with the dashed line that shows $N(E)$ for our earlier small-basis calculation [11] (276 states), and the dotted line for the present calculation (1433 states). The improvement is obvious, however, the agreement is not perfect. We believe that the remaining disagreement is not due to some missing configurations in the CI calculation, but rather due to an overall ''softening'' of the spectra due to screening of the Coulomb repulsion between the valence electrons by the electrons of the core [22]. In the CI language this effect is produced by the high-energy excitations of the valence electrons into the continuum together with the electron excitations from the core.

Two typical features can be observed in the spectra of complex atoms [6]. The first, clearly seen in Fig. 1, is the rapid increase of the level density $\rho(E)$ with energy [23]. Its origin is purely combinatorial — the larger the excitation energy, the greater the number of ways it can be distributed among a few single-particle excitations. In the independent-particle model this dependence is described by the following exponent [2]:

$$\rho_a(E)=\rho_0\,\exp(a\sqrt{E-E_g}), \tag{12}$$

where ρ_0 and a are some constants, and E_g is the ground-state energy of the system. This dependence also follows from the thermodynamic definition of the temperature, $T^{-1}=d\{\ln[\rho(E)]\}/dE$, combined with the estimates of the average number of excited Fermi particles, $n_{\rm ex}\propto T$, and that of the excitation energy, $E-E_g\sim n_{\rm ex}T$. The experimental spectra of rare-earth atoms and their ions examined in Ref. [6] are in agreement with Eq. (12).

Figure 1 shows that the calculated cumulative level number plot is fitted well by

$$N(E)=\int_{E_g}^{E}\rho_a(E')dE', \tag{13}$$

with $\rho_0=0.65$ eV^{-1}, $a=2.55$ eV$^{-1/2}$, and the ''ground state'' energy of the 4^+ sequence E_g shifted by 0.25 eV up from the true $J^\pi=4^-$ ground state of Ce. Thus Eq. (12) gives a good overall fit of the calculated level density below 6 eV.

The second feature typical for the spectra of complex many-body systems is level repulsion. It is a basic quantum mechanics fact that two levels with identical quantum numbers cannot be degenerate if they are coupled by nonzero matrix elements — they ''repel'' each other. In quantum chaotic systems, this repulsion is characterized by the Wigner level spacing distribution

$$P(s)=\frac{\pi s}{2}e^{-\pi s^2/4}, \tag{14}$$

where s is the nearest-neighbor level spacing normalized so that $\overline{s}=\int sP(s)ds=1$. Equation (14) shows that the probability of finding small level spacings is indeed vanishingly small. As we pointed out in Sec. I, spectral statistics do not tell much about the eigenstates of the system. However, Eq. (14) is still a good test for some possible hidden quantum numbers, e.g., the total spin or orbital momentum, which might characterize atomic eigenstates besides J^π. If these do exist, small level spacings (''degeneracies'') will be more abundant than predicted by Eq. (14). These statistics were checked for many experimental [5,6,11,16,18] and calculated [11,17] complex atomic spectra, as well as for molecular vibronic spectra [24].

As seen from Fig. 1 the level density changes significantly for the first 500 levels of the calculated spectrum. To analyze the distribution of the corresponding level spacings we use the analytical density fit $\rho_a(E)$ to normalize the spacings:

$$s_n=(E_{n+1}-E_n)\rho_a(E_n). \tag{15}$$

Their distribution shown on the inset in Fig. 1 is in reasonable agreement with the Wigner formula. The deviations are probably due to the long-range fluctuations of the level density, not accounted for by the simple exponential (12). In the previous calculation [11], where only the lowest orbitals of each symmetry were included, we also observed the Wigner distribution. When orbitals with higher principal quantum numbers become involved (as seen from Fig. 1 above 3.5 eV), the spatial extent of the eigenstates increases. This should cause a decrease of the residual Coulomb interaction

between the electrons. On the other hand, the level spacings also become smaller. As a result, the state mixing at these excitation energies remains strong, which is confirmed by the agreement with the Wigner distribution, and the eigenstates are chaotic. Our estimate of the number of principal components N shows that it becomes even greater as the energy increases, in accord with the estimate $N\sim\Gamma/D\sim 300$ ($\Gamma\sim 1$ eV, and the mean level spacing $D\approx 0.003$ eV at $E\approx 6$ eV).

B. Dipole matrix elements

In Sec. II, we explained that matrix elements involving chaotic compound states should have Gaussian statistics, and the mean squared value of the matrix elements could be estimated in terms of some average characteristics of the compound states. In this section, we concentrate on the dipole matrix elements ($E1$ amplitudes) $d_{ik}=\langle \Psi_i^{4^+}\|\hat{D}\|\Psi_k^{4^-}\rangle$ between the 14 lowest states with $J^\pi=4^-$ and 80 consecutive 4^+ states obtained numerically in our CI calculations of Ce. We have chosen this energy region to cover the range explored in the experiment [15], where absolute values were derived for 228 of the most intense lines of neutral Ce between 10 706 and 22 184 cm^{-1}.

Of course, low-lying atomic states, e.g., the ground state, have a well-defined configuration composition and are not chaotic; hence the $E1$ amplitudes between them should not be distributed in any particular statistical way. However, the matrix elements (2) will become random (and close to Gaussian) as soon as at least one of the states involved, the initial or the final, moves into the compound-state energy range and becomes a superposition of many random components. Besides that, the mean-squared value of the matrix element is expected to show some smooth secular variation with the energy of the states involved. For these reasons we skip the first 20 states with $J^\pi=4^+$, and analyze the statistics of the $14\times 80=1120$ $E1$ amplitudes for the following 80 even states by grouping them in bunches of 20 — 21–40, 41–60, 61–80, and 81–100 — which correspond to the mean excitation energies of 2.49, 2.95, 3.40, and 3.70 eV above the atomic ground state (the mean energy of the lowest 14 odd states is 0.68 eV). Thus each plate in Fig. 2 shows the distribution of the 280 reduced dipole matrix elements together with their rms value. Also shown in Fig. 2 are the Gaussian distributions $g(d)=\exp(-d^2/2d_0^2)/\sqrt{2\pi d_0^2}$, where the rms parameter d_0 has been adjusted to minimize χ^2 around the center of the histogram. The values of d_0 and χ^2 are given in Table I.

Two effects can be seen in Fig. 2. First, the distributions of the matrix elements are indeed close to Gaussian. Second, the width of the distributions (the mean-squared value of the matrix elements) varies with the energy of the even states. It is mostly this effect that is responsible for the visible discrepancies between the histograms and the Gaussian fits. To eliminate it, we can use a running average procedure to normalize the amplitudes,

$$d_{ik}^{(n)}\equiv\frac{d_{ik}}{\langle d^2\rangle_i^{1/2}}, \tag{16}$$

where $\langle d^2\rangle_i^{1/2}$ is the rms value over the 14 odd states, calculated for every even state i. Figure 3 confirms that the 1120 normalized $E1$ amplitudes for the 21–100 even states are distributed according to the normal law. The inset shows the dependence of the rms $E1$ amplitude $\langle d^2\rangle_i^{1/2}$ on the energy of the even state $E^{(i)}$. Fluctuations aside, it is in agreement with the rms values calculated from the statistical theory [Eq. (8)] at the energies of the 30th, 50th, 70th, and 90th even states. The numerical values of the rms $E1$ amplitudes are listed in Table I.

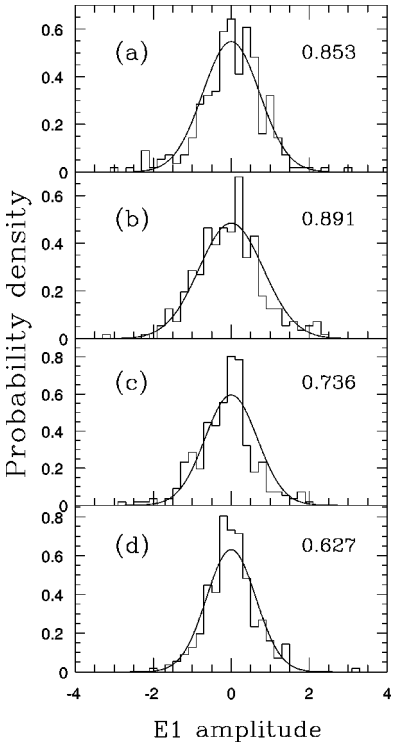

FIG. 2. Probability distributions of the $E1$ amplitudes in Ce for transitions between the 14 lowest 4^- states and groups of 20 states with $J^\pi=4^+$: (a) 21–40, (b) 41–60, (c) 61–80, and (d) 81–100. rms values of the amplitudes are shown next to the histograms. Smooth curves are Gaussian fits that minimize χ^2 for 21–17 central bins of the histograms (see Table I).

Note that we have chosen Eq. (8) with 1 standing for the odd states and 2 for the even ones. In our numerical example we consider the dependence of the rms $E1$ amplitude on the energy of the even states, and keep the odd states the same.

TABLE I. Root-mean-square $E1$ amplitudes for transitions between the 14 $J^\pi=4^-$ and 80 $J^\pi=4^+$ states in Ce.

	rms $E1$ amplitudes (a.u.)				
even levels	$(\overline{d_{ik}^2})^{1/2}$ [a]	from Eq. (8) [b]	d_0 [c]	n [d]	$\chi^2(n-1)$
21–40	0.853	0.813	0.729	21	24.4
41–60	0.891	0.746	0.824	21	23.9
61–80	0.736	0.674	0.671	17	36.6
81–100	0.627	0.566	0.632	17	24.7

[a]Obtained directly from the CI calculation.
[b]Calculated from the statistical theory, Sec. II.
[c]Values that minimize χ^2 for the Gaussian fits shown in Fig. 2.
[d]Number of bins around the center of the histogram used for calculation of χ^2.

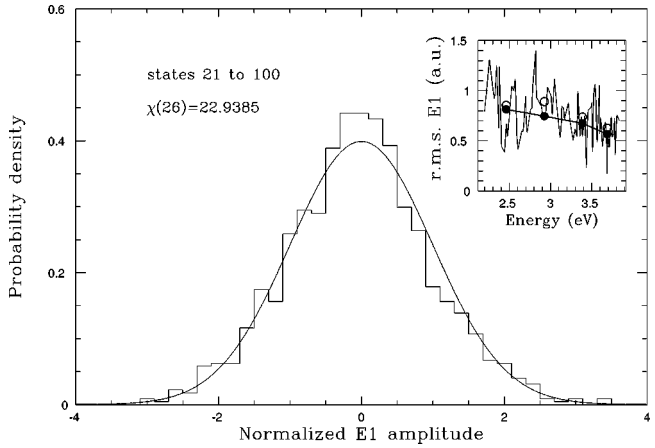

FIG. 3. Probability distributions of the normalized $E1$ amplitudes in Ce for transitions between the 14 lowest 4^- states and 21–100 states with $J^\pi=4^+$, compared to the normal distribution (solid line). The inset shows the dependence of the rms $E1$ amplitude averaged over the 14 odd states on the energy of the even state (thin solid line). Solid circles connected by a thick solid line are the rms values of the $E1$ amplitude obtained from the statistical theory [Eq. (8)] at the energies of the 30th, 50th, 70th, and 90th even states, and open circles are values from the CI calculation (see Table I).

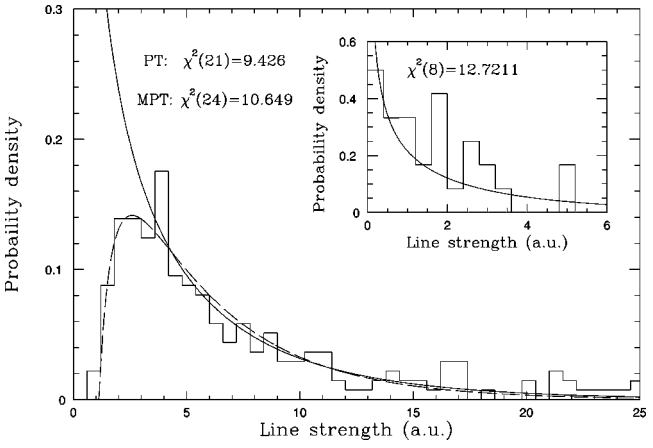

FIG. 4. Comparison of the line strengths measured in Ce by Bisson *et al.* [15] with the Porter-Thomas and modified Porter-Thomas distributions. The solid line is the PT distribution (20) with $A=2.07$ and $\overline{S}=3.3$ a.u., and the dashed line is the modified PT distribution (21) with $A=6.22$, $S_0=1.12$, and $\overline{S}=2.4$ a.u. Shown in the inset is the probability distribution of the 30 lines measured from branching ratios and delayed photoionization, fitted by a PT distribution with $\overline{S}=2.15$ a.u.

Therefore, as in Eq. (8), we only need to know the average occupation numbers for the lowest 14 odd states, and the result depends on the final even state via its energy $E^{(2)}$, mean level spacing D_2, and spreading width Γ_2. As we saw in our previous calculations [11], the even states of Ce with $J=4$ become very much chaotic at excitation energies of just 2 eV, i.e., from the 20th level up. Also, as earlier in Ref. [11], we use average configuration energies rather than single-particle Hartree-Fock energies to determine the transition frequencies $\omega_{n'l'j,nlj}$ needed for calculation of Δ in Eq. (8). The ground state of Ce is described as $4f6s^25d$; however, the dominant configuration among the 14 lowest odd states is $4f6s5d^2$, and we used it to calculate the transition energies. For example, the energy of the $6s$-$6p$ transition $\omega_{6p,6s}$ was determined as the difference between the average energies of the $4f5d^26p$ and $4f6s5d^2$ configurations. Physically, this corresponds to choosing a particular mean field close to that of the low-lying odd states of Ce for calculation of the transition energies. It should be mentioned, however, that the results obtained with the Hartree-Fock frequencies $\omega_{nlj,n'l'j'}=\epsilon_{nlj}-\epsilon_{n'l'j'}$ were not too different.

Gaussian statistics of the dipole matrix elements result in the Porter-Thomas (PT) distribution of the line strengths $S(i,k)=d_{ik}^2$,

$$f(S)=\frac{1}{\sqrt{2\pi S\overline{S}}}\exp\left(-\frac{S}{2\overline{S}}\right), \tag{17}$$

where $\overline{S}$ is the mean line strength. Divergence of this function at small S means that if the $E1$ amplitudes are Gaussian, there should be many weak lines in the spectrum. Earlier evidence of the PT statistics of line strengths can be found in calculations of dipole excitations in complex atoms [25], and transitions between the vibronic levels in molecules measured in Ref. [24].

IV. ANALYSIS OF EXPERIMENTAL DATA

In Ref. [15] absolute values of gA were obtained for 228 of the most intense observed lines between 10 706 and 22 184 cm^{-1} in Ce. It is interesting to analyze these data to see whether they support our theoretical and numerical considerations.

The values of gA listed in Ref. [15] are defined as $gA=(2J_k+1)A_{ki}$, where

$$A_{ki}=\frac{4e^2\omega_{ki}^3}{3\hbar c^3(2J_k+1)}|\langle i\|\hat{D}\|k\rangle|^2 \tag{18}$$

is the $E1$ transition rate from the upper level k into the lower level i [26]. We use the experimental values of gA and J_k and transition frequencies ω_{ki} to extract values of the line strengths

$$S(i,k)\equiv|\langle i\|\hat{D}\|k\rangle|^2=gA\frac{3\hbar c^3}{4e^2\omega_{ki}^3}. \tag{19}$$

In Fig. 4, the probability distribution of the 228 experimental line strengths is shown. Compared to the expected PT formula (17), there is a clear lack of small line strengths. Nevertheless, the decreasing part of the histogram can be fitted well by a PT distribution with an additional normalization factor A,

$$f_A(S)=\frac{A\,\exp(-S/2\overline{S})}{\sqrt{2\pi S\overline{S}}}, \tag{20}$$

shown in Fig. 4 by a solid line for $A=2.07$ and $\overline{S}=3.3$ a.u. that minimize χ^2 for the 22 bins with $S>3$ a.u.

It would be tempting to say that the excellent agreement between the PT curve and the histogram is a confirmation of the Gaussian statistics of the $E1$ amplitudes in Ce. The value of A would then indicate that about one-half of all lines are missing in the experimental data. However, the value of $\overline{S}=3.3$ a.u. corresponds to the rms $E1$ amplitude of 1.8, which is more than two times greater than our numerical results in Figs. 2 and 3 (inset), and in Table I. On the other hand, the experimentally observed 228 lines include transitions between levels with various total angular momenta between $J=1$ and 8 ($|J_i-J_k|\leqslant 1$, of course) whereas we have about 500 hundred lines with just $J_i=J_k=4$ in our calculation in the analogous energy range. This means that in Ref. [15] only the strongest 10% or less of all lines have in fact been measured. The very suggestive agreement with the PT distribution in Fig. 4 should then be considered as merely fortuitous.

It is worth noting that in experiment the lines are selected by their intensities proportional to gA, rather than strengths. Hence even lines with large strengths can be omitted if their frequencies are small. Let us look at the simplest model of this effect and see how it influences the observed strength distribution. Assume that transitions in a certain frequency range $0<\omega<\omega_{\max}$ are studied, and different values within this interval are equally probable. The observed intensities of the lines are proportional to $\omega^3 S$. If we assume that there is a minimal threshold intensity that can be registered, the original PT distribution of strengths would be modified as follows:

$$f_1(S) = \begin{cases} 0, & S\leqslant S_0 \\ \dfrac{A}{\sqrt{2\pi S\overline{S}}}\exp\left(-\dfrac{S}{2\overline{S}}\right)\left[1-\left(\dfrac{S_0}{S}\right)^{1/3}\right], & S>S_0, \end{cases} \tag{21}$$

where S_0 is the minimal strength that can be observed at $\omega=\omega_{\max}$, and A is the normalization factor. As seen from Fig. 4, Eq. (21) also gives a very good fit of the experimental data with $\overline{S}=2.4$, $S_0=1.12$, and $A=6.22$ [27]. Note, however, that the value of the mean line strength is 1.5 times smaller than the one we had from the pure PT fit. Therefore, the assumptions used in our processing of the experimental data affect the estimates of the experimental rms $E1$ amplitudes, and we should not be too concerned about the apparent disagreement with our numerical calculations. In addition, extraction of absolute line strengths from the experimental data is not free from uncertainties estimated in Ref. [15] at 10–20 %.

For 30 transitions in Ce, the gA values were obtained more accurately from branching ratios and delayed photoionization measurements of lifetimes (Ref. [15], Table 2). When we look at the statistics of the corresponding line strengths (Fig. 4, inset), and compare it with the PT distribution (17), a value of $\overline{S}=2.15$ is obtained, much smaller than the estimates of $\overline{S}$ from the statistics of the 228 lines. Thus it appears that to make firm conclusions about Gaussian statistics of the $E1$ amplitudes, a much more thorough experimental survey is needed. On the other hand, even relative measurements of a large number of line strengths could be very valuable for examining these statistics [24].

V. CONCLUSIONS

In this work, we have extended the configuration-interaction approach of Ref. [11] to calculate large numbers of eigenstates in Ce. In agreement with our earlier studies, the energy-level statistics indicate that the simple configurational basis states are strongly mixed together by the residual electron interaction, and the only good quantum numbers in the spectrum are parity and the total angular momentum. The total orbital momentum L and spin S are not conserved due to the spin-orbit interaction, whose effect is dynamically enhanced, just as that of any other perturbation in a chaotic many-body system [11].

The strong configuration mixing makes multielectron atomic eigenstates chaotic. This in turn results in a Gaussian statistics of the matrix elements for chaotic atomic eigenstates (compound states). This understanding is fully confirmed by our numerical calculations of the 1120 $E1$ amplitudes between the 14 lowest $J^\pi=4^-$ states and 80 $J^\pi=4^+$ states above 2 eV. It is important that the parameter of the Gaussian, the rms $E1$ amplitude, varies slowly with the excitation energy. This effect should be taken into account when analyzing the statistics of the matrix elements.

We also show that a statistical theory can be used to estimate mean-squared matrix elements involving compound states. It enables one to express the answer in terms of the single-particle matrix elements and occupation numbers, and parameters of the compound states, namely, the number of principal components and the spreading width. This approach has already been applied to a calculation of matrix elements between compound states in nuclei [14]. It could be useful in various other many-body systems, e.g., atomic clusters or quantum dots, where direct diagonalization of the Hamiltonian matrix is not feasible because of a huge size of the Hilbert space of the problem.

An attempt has been made to analyze existing experimental data for the line strengths in Ce [15]. It appears that the statistics of the measured line strengths is compatible with the Porter-Thomas distribution, with allowance for the missing weak lines. However, the discrepancy between the calculated rms $E1$ amplitudes and those inferred from the experimental data does not allow us to say that the existence of quantum chaos in the Ce eigenstates has been confirmed experimentally. To make this statement, one would have to do a much more complete survey and statistical analysis of the line strengths in the Ce spectrum.

On the other hand, this means that a comparison between the experimental and theoretical line strengths in Ce is not yet possible, even at the level of their mean values. Theoretically, to calculate precisely the dipole matrix elements between particular levels in the compound-state energy range of complex atoms like Ce looks like a prohibitively difficult

problem. Experimentally, identification of specific lines in enormously complicated spectra is also a very difficult task. However, we would like to suggest that extraction of mean characteristics from the experiment and comparison with the corresponding theoretical estimates is a meaningful way of exploring such complex systems. As a result, one might hope to obtain a deeper insight into the existence of quantum chaos in many-body systems on the whole, and in complex open-shell atoms, in particular.

ACKNOWLEDGMENTS

We would like to thank O. P. Sushkov for useful discussions, and acknowledge support of this work by the Australian Research Council.

[1] *Quantum Chaos: Between Order and Disorder*, a selection of papers compiled and introduced by G. Casati and B. V. Chirikov (Cambridge University Press, Cambridge, 1995), Pt. 2; see also M. Courtney and D. Kleppner, Phys. Rev. A **53**, 178 (1996), and references therein.

[2] A. Bohr and B. Mottelson, *Nuclear Structure* (Benjamin, New York, 1969), Vol. 1.

[3] T. A. Brody, J. Flores, J. B. French, P. A. Mello, A. Pandey, and S. S. M. Wong, Rev. Mod. Phys. **53**, 385 (1981).

[4] T. Guhr, A. Müller-Groeling, and H. A. Weidenmüller, MPI preprint H V27 1997; cond-mat/9707301.

[5] N. Rosenzweig and C. E. Porter, Phys. Rev. **120**, 1698 (1960).

[6] H. S. Camarda and P. D. Georgopulos, Phys. Rev. Lett. **50**, 492 (1983).

[7] D. Delande and J. C. Gay, Phys. Rev. Lett. **57**, 2006 (1986).

[8] M. V. Berry, Ann. Phys. (N.Y.) **131**, 163 (1981); O. Bohigas, M. J. Giannnoni, and C. Schmit, Phys. Rev. Lett. **52**, 1 (1983).

[9] B. V. Chirikov, Phys. Lett. **108A**, 68 (1985).

[10] *Atomic Energy Levels — The Rare-Earth Elements*, edited by W. C. Martin, R. Zalubas, and L. Hagan, Natl. Bur. Stand. (U.S.) Ref. Data Ser. No. NBS-60 (U.S. GPO, Washington, DC, 1978).

[11] V. V. Flambaum, A. A. Gribakina, G. F. Gribakin, and M. G. Kozlov, Phys. Rev. A **50**, 267 (1994).

[12] A. A. Gribakina, V. V. Flambaum, and G. F. Gribakin, Phys. Rev. E **52**, 5667 (1995).

[13] V. V. Flambaum, A. A. Gribakina, and G. F. Gribakin, Phys. Rev. A **54**, 2066 (1996).

[14] V. V. Flambaum and O. K. Vorov, Phys. Rev. Lett. **70**, 4051 (1993); V. V. Flambaum, in *Time Reversal and Parity Violation in Neutron Reactions*, edited by C. R. Gould, J. D. Bowman, and Yu. P. Popov (World Scientific, Singapore, 1994), p. 39.

[15] S. E. Bisson, E. F. Worden, J. G. Conway, B. Comaskey, J. A. D. Stockdale, and F. Nehring, J. Opt. Soc. Am. B **8**, 1545 (1991).

[16] J. P. Connerade, M. A. Baig, and M. Sweeney, J. Phys. B **23**, 713 (1990).

[17] J. P. Connerade, I. P. Grant, P. Marketos, and J. Oberdisse, J. Phys. B **28**, 2539 (1995).

[18] J. P. Connerade, J. Phys. B **30**, L31 (1997).

[19] N. Vaeck and N. J. Kylstra (unpublished).

[20] If the number of active electrons in the system is more than two, the Hamiltonian matrix H_{jk} appears to be sparse, i.e., there is a certain fraction of zero off-diagonal matrix elements in it (only the basis states that differ by the positions of no more than two electrons can be coupled by the two-body Coulomb interaction). In this case, one should compare the magnitude of H_{jk} with the mean ''distance'' $|E_k-E_j|$ between the basis states directly coupled by nonzero H_{jk}. See, e.g., P. Jacquod and D. L. Shepelyansky, Phys. Rev. Lett. **79**, 1837 (1997); B. Georgeot and D. L. Shepelyansky, *ibid*. **79**, 4365 (1997), and references therein.

[21] There are some specific correlations caused by the two-body character of the electron interaction, but they do not change the statistics of the matrix elements. However, they can influence the estimate of the mean-square value of the matrix element; see V. V. Flambaum, G. F. Gribakin, and F. M. Izrailev, Phys. Rev. E **53**, 5729 (1996).

[22] See, e.g., V. A. Dzuba, V. V. Flambaum, and M. G. Kozlov, Phys. Rev. A **54**, 3948 (1996), and references therein.

[23] Note that there are no Rydberg series in our CI calculation for Ce, and only the s, p, d, and f orbitals with the two lowest principal quantum numbers are considered. Of course, the inclusion of single-particle Rydberg excitation series would give infinite density peaks at the positive ion thresholds. However, the extended large-radius Rydberg states are physically different from the compact compound states, and they decouple from the compound state spectra at high n; A. A. Gribakina and G. F. Gribakin, J. Phys. B **29**, L809 (1996).

[24] Th. Zimmermann, H. Köppel, L. S. Cederbaum, G. Persch, and M. Demtröder, Phys. Rev. Lett. **61**, 3 (1988).

[25] R. Karazija, *Sums of Atomic Quantities and Mean Characteristics of Spectra* (Mokslas, Vilnius, 1991).

[26] I. S. Sobelman, *Atomic Spectra and Radiative Transitions* (Springer-Verlag, Berlin, 1992).

[27] The normalization integral $\int f_1(S)dS$ for this set of values is equal to 0.902, as this fit, just like the pure PT fit, evidently fails to describe the large number of line strengths greater than 15 a.u. observed in Ref. [15].